J. Fluid Mech. (1973), vol. 58, part 1, pp. 197–205
Printed in Great Britain

Propagation of spherical and cylindrical N-waves

By P. L. SACHDEV† AND R. SEEBASS
Graduate School of Aerospace Engineering, Cornell University, Ithaca, N.Y.

(Received 3 October 1972)

An implicit predictor–corrector difference scheme is employed to study the propagation of spherical and cylindrical N-waves governed by the modified Burgers equation

$$\frac{\partial u}{\partial t}+u\frac{\partial u}{\partial x}+\frac{\nu u}{2t}=\frac{\delta}{2}\frac{\partial^2 u}{\partial x^2},$$

where $\nu = 0$, 1 or 2 for plane, cylindrical and spherical symmetry respectively. The numerical scheme is first tested by computing the plane solution and comparing it with the exact analytic solution obtained by Lighthill (1956) through the Hopf–Cole transformation.

Our numerical solutions for the non-planar N-waves show that variation of the 'lobe' Reynolds number, which may be used as a measure of the importance of viscous diffusion, can be accurately determined by the analysis which is strictly valid only for large Reynolds numbers. This is true even when shock wave is well diffused and the 'lobe' Reynolds number is as small as $\frac{1}{2}$.

1. Introduction

A simple equation describes the motion of weak nonlinear waves in gases when the dissipative effects are taken into account. This equation was probably first mentioned by Bateman (1915) with reference to certain fluid motions. Burgers (1948) proposed this equation as a model for one-dimensional turbulence and subsequently it has been called the Burgers equation. Lighthill, in his 1956 survey paper, derived the equation from the basic equations of gasdynamics in the form

$$\frac{\partial u}{\partial t}+u\frac{\partial u}{\partial X}=\frac{\delta}{2}\frac{\partial^2 u}{\partial X^2}, \tag{1.1}$$

where u is the excess wave velocity, $u = v+a-a_0$, v and a being the particle and sound speed respectively; $X = x-a_0t$ is a co-ordinate measured in a frame of reference which moves in the same direction as the wave at the undisturbed speed of sound a_0; x and t are, of course, space and time co-ordinates. The co-ordinate X enables us to follow changes in the wave form without further changes in the origin. The coefficient δ is the 'diffusivity of sound', being a combination of different diffusivities which affect acoustic attenuation.

Equation (1.1) represents a balance between convection and viscous diffusion. It follows from the assumption that the ratio U/a, of the maximum fluid velocity to the speed of sound and the viscous diffusivity, non-dimensionalized by an effective frequency ω chosen such that $U\omega/a$ is the maximum velocity gradient,

† Present address: Department of Applied Mathematics, Indian Institute of Science, Bangalore–560012.

are small and of the same order. The variant of this equation that applies for motion with plane, cylindrical and spherical symmetry is

$$\frac{\partial u}{\partial t}+u\frac{\partial u}{\partial X}+\frac{\nu u}{2t}=\frac{\delta}{2}\frac{\partial^2 u}{\partial X^2}, \tag{1.2}$$

where $\nu = 0$, 1 or 2 for plane, cylindrical and spherical symmetry respectively. The other variables have the same significance as in (1.1). Leibovich & Seebass (1972) discussed in some detail the relative role of nonlinearity and viscous dissipation in the entire course of evolution of a wave produced initially by a plane, cylindrical or spherical piston. The formation of an N-wave from an initial wave form with both positive and negative phases and its subsequent decay were also discussed for large and small Reynolds numbers respectively.

In plane geometry ($\nu = 0$) equation (1.2) fortunately admits a transformation $u = -\delta(\phi_x/\phi)$, discovered by Hopf (1950) and Cole (1951), which renders this equation linear; indeed, it becomes the well-known heat equation in ϕ. Lighthill (1956) deduced a number of useful results for weak plane shock waves by using the above transformation. In particular, he studied the decay of a 'balanced' N-wave for which

$$\int_{-\infty}^{\infty} u\,dX = 0.$$

This wave may be produced by moving a piston forward and then returning it to its original position. For an N-wave, a convenient precise definition of the Reynolds number is

$$R = \frac{1}{\delta}\int_0^{\infty} u\,dX,$$

which is the ratio of the product of velocity amplitude and length scale of the front 'lobe' of the N-wave to the diffusivity δ. Thus initially, with δ a small quantity, $R \gg 1$, the viscous term in (1.2) is important only in the thin shock layer, and the solution in the inviscid region is $u = X/t$, which is shape-preserving. On integrating (1.2) with respect to X from 0 to ∞ and making use of the slope at $X = 0$ from the inviscid solution, one finds that $R \sim \ln(t_0/t)$, where t_0 is a constant. On the other hand, when the wave has propagated a long distance and nonlinearity is no longer important, the solution becomes essentially diffusive, and it can easily be shown that $R \sim (t_0/t)^{\frac{1}{2}}$, where t_0 is (different) constant. Lighthill (1956) obtained the exact solution as $R = \ln[1+(t_0/t)^{\frac{1}{2}}]$, where t_0 is a time when the pulse length has become a large multiple of its initial value. It is obvious that this solution has the asymptotic behaviour referred to above.

It is of some interest to study the decay of spherical and cylindrical N-waves, which find applications, for example, in explosions and the theory of the sonic boom from an aircraft. Equation (1.2) for $\nu = 1, 2$ does not admit a Hopf–Cole type of transformation and hence has to be dealt with in its nonlinear form. An approximate analytic solution of the problem will be reported later. In the present paper we study the spherical and cylindrical N-waves numerically using an implicit predictor–corrector scheme suggested by Douglas & Jones (1963). Section 2 gives the difference scheme employed to solve (1.2) and the details of the numerical procedure. Section 3 contains the test calculations for the plane

N-wave and a comparison with the exact analytic solution obtained by Lighthill (1956). Section 4 deals with the spherical and cylindrical N-waves, and finally §5 provides the conclusions of this study.

2. Difference scheme and numerical procedure

Equation (1.2) belongs to the general class of nonlinear parabolic equations

$$u_{XX} = F(X, t, u, u_X, u_t). \tag{2.1}$$

Douglas & Jones (1963) suggested an implicit predictor–corrector form of the difference scheme given by

$$\left.\begin{aligned} \Delta_X^2 u_{i,j+\frac{1}{2}} &= F[X_i, t_{j+\frac{1}{2}}, u_{i,j}, \delta_X u_{i,j}, (u_{i,j+\frac{1}{2}} - u_{i,j})/\tfrac{1}{2}k] \quad \text{(predictor)},\\ \tfrac{1}{2}\Delta_X^2(u_{i,j+1} + u_{i,j}) &\\ &= F[X_i, t_{j+\frac{1}{2}}, u_{i,j+\frac{1}{2}}, \tfrac{1}{2}\delta_X(u_{i,j+1} + u_{i,j}), (u_{i,j+1} - u_{i,j})/k] \quad \text{(corrector)},\end{aligned}\right\} \tag{2.2}$$

where

$$\left.\begin{aligned} \Delta_X^2 u_{i,j} = h^{-2}(u_{i+1,j} - 2u_{i,j} + u_{i-1,j}), \quad \delta_X u_{i,j} = (2h)^{-1}(u_{i+1,j} - u_{i-1,j}),\\ u_{i,j} = u(X_i, t_j), \quad X_i = ih, \quad t_j = jk.\end{aligned}\right\} \tag{2.3}$$

This difference scheme has a truncation error of $O(h^2 + k^2)$, where h and k are space and time mesh sizes respectively. Douglas & Jones (1963) have demonstrated the convergence of the difference scheme (2.2) for (2.1). At any two consecutive times $t_{j+\frac{1}{2}}$ and t_{j+1}, separated by a time interval $\frac{1}{2}k$, this scheme leads to two sets of linear algebraic equations in the unknowns $u_{i,j+\frac{1}{2}}$ and $u_{i,j+1}$, which reduce to a triadiagonal matrix form provided that we guess the value of u at the first of the set of points, both at $t_{j+\frac{1}{2}}$ and t_{j+1}. Assuming the initial values described in the following sections, the solution at the subsequent time is obtained by an iterative scheme that assumes that the solution at a few points on the left of the node of the N-wave is antisymmetric with respect to those on the right. This requires changing the value of u at the extreme left end-point at $t_{j+\frac{1}{2}}$ and t_{j+1} until the required antisymmetry condition is satisfied to the desired accuracy.

As the computation proceeds, the wave profile spreads to the right (and left) and new points have to be added at successive times, where the value of u is significant (say greater than 10^{-6}). As the pulse grows in length, say, becoming twice its original length, the mesh size is increased to keep the matrix of this system from becoming unwieldy. The calculations were repeated to ensure that the accuracy of the solution did not suffer by this change of mesh size.

If we substitute the difference scheme (2.2) with (2.3) in (1.2), we obtain

$$\left.\begin{aligned} &u_{i+1,j+\frac{1}{2}} - 2(1 + (2h^2/\delta k))\, u_{i,j+\frac{1}{2}} + u_{i-1,j+\frac{1}{2}}\\ &\quad = 2u_{i,j}\left[\frac{-2h^2}{\delta k} + \frac{h}{2\delta}(u_{i+1,j} - u_{i-1,j}) + \frac{\nu h^2}{2\delta(j+\frac{1}{2})k}\right] \quad \text{(predictor)},\\ &\left(1 - \frac{h}{\delta}u_{i,j+\frac{1}{2}}\right)u_{i+1,j+1} - 2\left(1 + \frac{2h^2}{k\delta}\right)u_{i,j+1} + \left(1 + \frac{h}{\delta}u_{i,j+\frac{1}{2}}\right)u_{i-1,j+1}\\ &\quad = \left(-1 + \frac{h}{\delta}u_{i,j+\frac{1}{2}}\right)u_{i+1,j} + 2\left(1 - \frac{2h^2}{\delta k}\right)u_{i,j} - \frac{h}{\delta}u_{i-1,j}u_{i,j+\frac{1}{2}}\\ &\qquad\qquad - u_{i-1,j} + \frac{2\nu h^2 u_{i,j+\frac{1}{2}}}{\delta k(j+\frac{1}{2})} \quad \text{(corrector)}.\end{aligned}\right\} \tag{2.4}$$

	$t = 3{\cdot}0,\ R = 2{\cdot}4859$ u		$t = 9{\cdot}0,\ R = 1{\cdot}9954$ u		$t = 29{\cdot}0,\ R = 1{\cdot}5123$ u	
X	Numerical	Exact	Numerical	Exact	Numerical	Exact
0	0	0	0	0	0	0
0·04	0·01220	0·01219	0·00384	0·00384	0·00108	0·00108
0·08	0·02423	0·02422	0·00765	0·00764	0·00215	0·00215
0·12	0·03588	0·03586	0·01140	0·01139	0·00321	0·00321
0·16	0·04685	0·04682	0·01506	0·01505	0·00426	0·00426
0·20	0·05669	0·05665	0·01858	0·01858	0·00530	0·00530
0·24	0·06471	0·06467	0·02193	0·02192	0·00631	0·00631
0·28	0·06994	0·06990	0·02504	0·02503	0·00730	0·00730
0·32	0·07114	0·07111	0·02784	0·02783	0·00826	0·00826
0·36	0·06715	0·06715	0·03025	0·03024	0·00918	0·00918
0·40	0·05777	0·05782	0·03216	0·03215	0·01006	0·01005
0·44	0·04454	0·04463	0·03348	0·03347	0·01088	0·01088
0·48	0·03055	0·03064	0·03408	0·03407	0·01166	0·01166
0·52	0·01873	0·01879	0·03387	0·03386	0·01237	0·01237
0·56	0·01040	0·01043	0·03278	0·03279	0·01301	0·01301
0·60	0·00531	0·00532	0·03083	0·03084	0·01357	0·01357
0·64	0·00252	0·00252	0·02808	0·02811	0·01404	0·01404
0·68	0·00112	0·00112	0·02472	0·02476	0·01442	0·01442
0·72	$0{\cdot}00467 \times 10^{-1}$	$0{\cdot}00467 \times 10^{-1}$	0·02101	0·02105	0·01469	0·01469
0·76	$0{\cdot}00184 \times 10^{-1}$	$0{\cdot}00186 \times 10^{-1}$	0·01722	0·01727	0·01485	0·01486
0·80	$0{\cdot}00684 \times 10^{-2}$	$0{\cdot}00697 \times 10^{-2}$	0·01363	0·01367	0·01490	0·01491
0·84	$0{\cdot}00314 \times 10^{-2}$	$0{\cdot}00322 \times 10^{-2}$	0·01043	0·01046	0·01483	0·01484
0·88			0·00773	0·00775	0·01463	0·01464
0·92			0·00556	0·00558	0·01432	0·01433
0·96			0·00390	0·00391	0·01388	0·01390
1·00			0·00266	0·00267	0·01334	0·01335
1·04			0·00178	0·00178	0·01270	0·01271
1·2			$0{\cdot}00283 \times 10^{-1}$	$0{\cdot}00284 \times 10^{-1}$	0·00943	0·00945
1·4			$0{\cdot}00164 \times 10^{-2}$	$0{\cdot}00184 \times 10^{-2}$	0·00519	0·00520
1·8					0·00810	0·00814
2·2					$0{\cdot}00611 \times 10^{-1}$	$0{\cdot}00638 \times 10^{-1}$

TABLE 1. Comparison of numerical and exact solutions for plane N-wave with initial values $R_i = 3$, $t_i = 1$, $t_0 = 364{\cdot}26$ at times $t = 3, 9, 29, 122, 347$

We mention here a comparative study of difference schemes for inviscid and viscous flows by Taylor, Ndefo & Masson (1972). It was found that the third-order implicit difference scheme of Rusanov (1961) with an explicit artificial viscosity provided the best results. The difference scheme used in the present paper is shown here to be a good alternative which is simple to use and does not require an artificial viscosity.

3. Test calculations: plane N-wave

As we noted in § 1, Lighthill (1956) obtained a closed-form solution for a plane ($\nu = 0$) balanced N-wave for which

$$\int_{-\infty}^{\infty} u\,dX = 0.$$

	$t = 122,\ R = 1{\cdot}0004$			$t = 531,\ R = 0{\cdot}603$	
	u			u	
X	Numerical	Exact	X	Numerical	Exact
0	0	0	0	0	0
0·04	0·000208	0·000208	0·2	0·000170	0·000170
0·08	0·000415	0·000415	0·4	0·000338	0·000338
0·12	0·000621	0·000622	0·6	0·000501	0·000502
0·16	0·000827	0·000828	0·8	0·000659	0·000660
0·20	0·00103	0·00103	1·00	0·000808	0·000809
0·24	0·00123	0·00124	1·20	0·000946	0·000948
0·28	0·00144	0·00144	1·40	0·00167	0·00107
0·32	0·00163	0·00164	1·60	0·00119	0·00119
0·36	0·00183	0·00183	1·80	0·00128	0·00128
0·40	0·00203	0·00203	2·0	0·00136	0·00136
0·44	0·00222	0·00222	2·2	0·00142	0·00143
0·48	0·00240	0·00240	2·4	0·00146	0·00147
0·52	0·00259	0·00259	2·6	0·00149	0·00149
0·56	0·00277	0·00277	2·8	0·00149	0·00150
0·60	0·00294	0·00294	3·0	0·00147	0·00148
0·64	0·00311	0·00311	3·2	0·00144	0·00145
0·68	0·00328	0·00328	3·4	0·00139	0·00140
0·72	0·00344	0·00344	3·6	0·00132	0·00133
0·76	0·00359	0·00359	3·8	0·00125	0·00125
0·80	0·00374	0·00374	4·0	0·00116	0·00117
0·84	0·00388	0·00388	4·2	0·00107	0·00108
0·88	0·00402	0·00402	4·4	0·000969	0·000978
0·92	0·00414	0·00415	4·6	0·000871	0·000879
0·96	0·00426	0·00427	4·8	0·000773	0·000781
1·00	0·00438	0·00438	5·0	0·000678	0·000687
1·04	0·00448	0·00448	5·4	0·000505	0·000513
1·4	0·00500	0·00501	5·8	0·000360	0·000368
1·8	0·00463	0·00463	6·2	0·000245	0·000253
2·2	0·00345	0·00346	6·4	0·000159	0·000168
2·6	0·00207	0·00208	6·8	$0{\cdot}00987 \times 10^{-1}$	0·000107
3·0	0·00101	0·00102	7·2	$0{\cdot}000575 \times 10^{-1}$	$0{\cdot}000662 \times 10^{-1}$
3·4	$0{\cdot}00409 \times 10^{-1}$	$0{\cdot}00415 \times 10^{-1}$	7·6	$0{\cdot}000308 \times 10^{-1}$	$0{\cdot}000394 \times 10^{-1}$
3·8	$0{\cdot}00137 \times 10^{-1}$	$0{\cdot}00144 \times 10^{-1}$	8·0	$0{\cdot}000143 \times 10^{-1}$	$0{\cdot}000227 \times 10^{-1}$
4·2	$0{\cdot}00350 \times 10^{-2}$	$0{\cdot}00431 \times 10^{-2}$	8·4	$0{\cdot}000475 \times 10^{-2}$	$0{\cdot}000127 \times 10^{-1}$

TABLE 1 (*Cont.*).

As noted by Lighthill, the Reynolds number

$$R = \frac{1}{\delta}\int_{X_n}^{\infty} u\,dX,$$

where X_n is the position of the node $u = 0$, is not invariant with time, as there is mass diffusion across the node, i.e. $u_x(0,t) \neq 0$. Lighthill's solution is

$$u = \frac{X/t}{1+\exp\left[X^2/2\delta t\right]/(e^R-1)} = \frac{X/t}{1+(t/t_0)^{\frac{1}{2}}\exp\left[X^2/2\delta t\right]}, \tag{3.1}$$

where R is the Reynolds number and is equal to $\ln\left(1+(t_0/t)^{\frac{1}{2}}\right)$.

t	1	25	49	75	99	125	151	175	201	301	531
Numerical	3·000	1·571	1·314	1·162	1·068	0·993	0·934	0·890	0·849	0·739	0·597
Exact	3·000	1·572	1·315	1·164	1·071	0·996	0·937	0·893	0·853	0·733	0·603

TABLE 2. Comparison of the values of Reynolds numbers at different (normalized) times as obtained from numerical and exact solutions for $\nu = 0$, $R_i = 3$, $t_i = 1$, $t_0 = 364{\cdot}26$

Before proceeding to the non-planar cases, we first reproduced the plane solution by our numerical procedure. The expression for the Reynolds number shows that it changes very slowly with time when it is large and decays like $(t_0/t)^{\frac{1}{2}}$ only when it becomes small. Therefore, we consider the solution over two different ranges of Reynolds number. At this point we recall that, in the Burgers equation, u, X and t are assumed to have been rendered non-dimensional by a_0, l and l/a_0, respectively, where a_0 is the (constant) ambient sound speed and l is a typical wavelength. The diffusivity δ is correspondingly normalized by $(a_0 l)^{-1}$. The initial non-dimensional time t is conveniently chosen to be 1 and the initial wave profile at this time is prescribed by its Reynolds number. The exact solution of Lighthill then determines the solution completely. If this solution were not known, we would proceed in the manner described in the following section for $\nu = 1$ and 2. We have considered two different cases: (i) initially, $R_i = 20$, $h = 0{\cdot}01, k = 0{\cdot}01$ and finally, $R_f = 18{\cdot}8, t_f = 11{\cdot}5$; (ii) $R_i = 3, h = 0{\cdot}01, k = 0{\cdot}01$. In case (ii) we proceeded until the wave profile became 'sufficiently' smooth ($t_f = 137$); we then doubled the space interval and carried on the computation until $R_f = 0{\cdot}6$ and $t_f = 531$.

The numerical calculations and the exact solutions are indistinguishable on any reasonable graph. Therefore, we compare the two solutions at different Reynolds numbers in table 1 for case (ii). The agreement is excellent everywhere except at the extreme ends of the N-wave, where the magnitude of u becomes very small and the prescribed accuracy (10^{-6}) is not sufficient to obtain accurate results (percentage-wise) in these regions. Throughout the calculations the wave is artificially truncated at the point where $|u| < 10^{-6}$. Table 2 compares the values of Reynolds numbers at different times obtained numerically with those from (3.2). As is to be expected, the agreement is again good, although there is a small error partly due to this truncation of the numerical solution at a finite distance.

4. Spherical and cylindrical N-waves

To obtain initial conditions for spherical and cylindrical N-waves, we make use of the discontinuous solutions

$$u = \begin{cases} \left.\begin{aligned} &\frac{X}{2t} \quad \text{for} \quad X \leqslant 1, \\ &0 \quad \text{for} \quad X > 1, \end{aligned}\right\} \quad \nu = 1, \\ \left.\begin{aligned} &\frac{X}{t \log t} \quad \text{for} \quad X \leqslant 1, \\ &0 \qquad \text{for} \quad X > 1, \end{aligned}\right\} \quad \nu = 2, \end{cases} \tag{4.1}$$

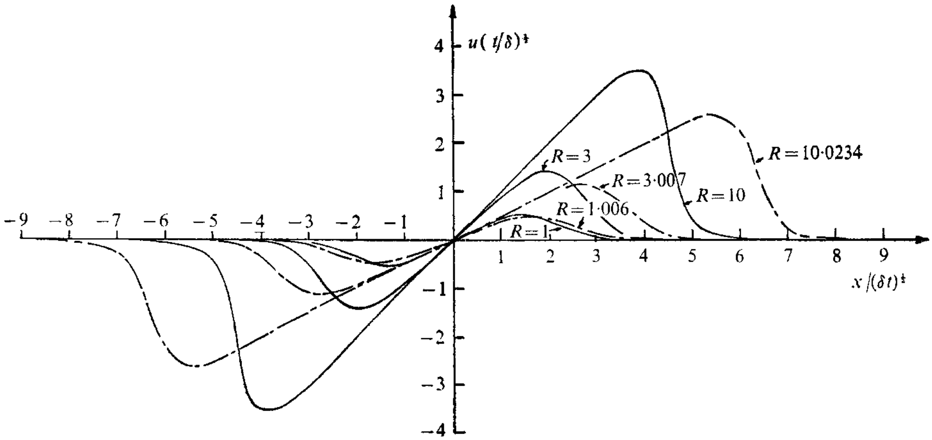

FIGURE 1. N-waves for Reynolds numbers $R = 10$, 3 and 1. ——, planar motion; —·—, cylindrical symmetry.

where $X = 1$ is taken to be a convenient position of the discontinuity. We impart structure to this discontinuity by using Taylor's shock structure for the plane case. This approximation is reasonably good for large Reynolds numbers as the non-planar shocks may be considered locally planar. Thus, in the thin shock layer,

$$u = \frac{u_{\max}}{1+\exp\left[u_{\max}(X-X_S)/\delta\right]}, \tag{4.2}$$

where $u_{\max}$ is the value of u at $X = 1$ and X_S is the centre of a thin shock such that it is situated half-way between the points where $u = 0{\cdot}95u_{\max}$ and $u = 0{\cdot}05u_{\max}$. The initial parameters for the two cases were selected so that the discontinuous profile had a Reynolds number equal to 20. This gives: (i) for $\nu = 1$, $u_{\max} = 0{\cdot}392$, $t_i = 1{\cdot}25$, $\delta = 0{\cdot}01$, $X_S = 1{\cdot}075$, $R_i = 23{\cdot}03$; (ii) for $\nu = 2$, $\delta = 0{\cdot}01$, $X_S = 1{\cdot}075$, $u_{\max} = 0{\cdot}392$, $t_i = 2{\cdot}61$, $R_i = 23{\cdot}03$. The space and time mesh sizes were chosen to be $h = 0{\cdot}01$ and $k = 0{\cdot}01$. The time mesh size was first selected to be $0{\cdot}005$ but a test calculation for 500 cycles showed that the accuracy was not affected by taking it to be $0{\cdot}01$. The linear profile in the inviscid region given by (4.1) was also calculated to serve as a check on the results because, for large Reynolds numbers, the solution in this region is given by (4.1). In both cases the computations were carried out until the Reynolds number had decreased to about $\frac{1}{3}$. Figures 1 and 2 give a comparison of the (normalized) solution for plane, cylindrical and spherical N-waves, having Reynolds numbers of 10, 3 and 1.

If we integrate (1.2) with respect to X from 0 to ∞, make use of the definition (3.2) for the Reynolds number and assume that the gradient of u with respect to X at the origin is given by equation (4.1), we obtain

$$R = \begin{cases} -\dfrac{1}{2}+\left(\dfrac{t_0}{t}\right)^{\frac{1}{2}} & \text{for} \quad \nu = 1; \\[2ex] \dfrac{c}{t}-\dfrac{1}{2t}\displaystyle\int_{t_i}^{t}\frac{dt}{\log t} & \text{for} \quad \nu = 2. \end{cases} \tag{4.3}$$

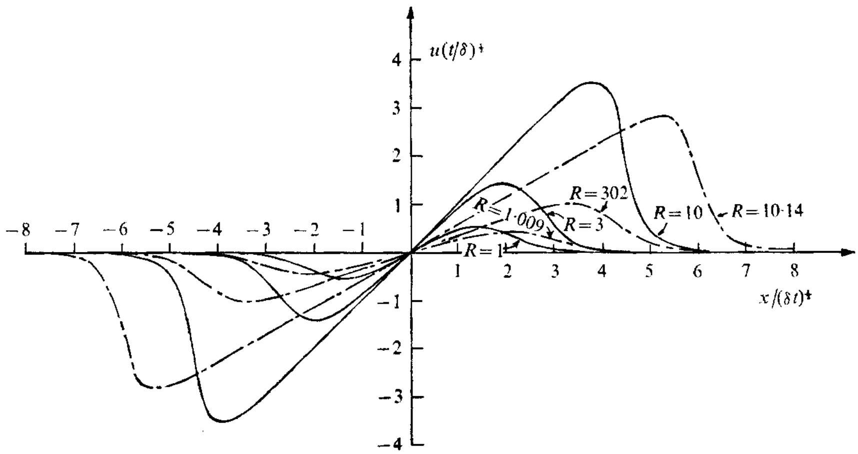

FIGURE 2. N-waves (asymptotic forms of pulses with zero mass flow) for Reynolds numbers R = 10, 3 and 1. ——, planar motion; —·—, spherical symmetry.

	$\nu = 1$			$\nu = 2$	
	R			R	
t	Numerical	Integral	t	Numerical	Integral
1·25	23·0306	23·0306	2·61	23·0306	23·0306
6·25	10·023	10·023	5·21	11·343	11·347
10·25	7·717	7·717	10·11	5·723	5·726
20·25	5·346	5·346	20·11	2·784	2·786
30·25	4·283	4·283	30·11	1·807	1·809
40·25	3·646	3·647	40·11	1·322	1·323
50·25	3·211	3·211	50·11	1·032	1·033
60·25	2·889	2·889	60·11	0·8395	0·840
70·25	2·638	2·639	70·11	0·703	0·703
80·25	2·436	2·437	80·11	0·601	0·601
90·25	2·269	2·269	90·11	0·523	0·522
100·25	2·127	2·127	100·11	0·460	0·459
150·25	1·647	1·646	110·11	0·410	0·407
200·25	1·361	1·359	120·11	0·368	0·365
311·25	1·001	0·991	130·11	0·333	0·329
441·25	0·772	0·752			
601·25	0·606	0·573			
801·25	0·479	0·429			
1001·25	0·396	0·331			

TABLE 3. Comparison of the values of Reynolds numbers at different (normalized) times as obtained from the numerical solution and the integral (4.2); $R_i = 23{\cdot}0306$ and $t_i = 1{\cdot}25$ for $\nu = 1$, and $R_i = 23{\cdot}0306$ and $t_i = 2{\cdot}61$ for $\nu = 2$.

Here we evaluate the constants t_0, c and t_i by making use of the initial conditions. Thus, for $\nu = 1$ with $t_i = 1{\cdot}25$ and $R_i = 23{\cdot}03$, we have $t_0 = 692{\cdot}08$ and for $\nu = 2$ with $t_i = 2{\cdot}61$ and $R_i = 23{\cdot}03$, c is found to be equal to $60{\cdot}109$. Making use of these constants we evaluate the Reynolds number at subsequent times. Table 3 compares the values of the Reynolds number obtained from the numerical solution with those obtained from (4.3). In both cases the agreement is excellent for $R > \frac{1}{2}$. We arrive at the important conclusion that the 'lobe' Reynolds number of the spherical and cylindrical N-waves may be obtained from (4.2) for the entire time regime over which it decreases from a large value to a value as low as $\frac{1}{2}$. This is possible because the slope of the wave profile at the origin is correctly given by equation (4.1) even when the N-wave has propagated a long distance and has diffused markedly.

5. Conclusions

We have studied the propagation of spherical and cylindrical N-waves numerically. An implicit predictor–corrector method is used to solve an initial boundary-value problem over an infinite domain and provides excellent results. An important result of this numerical study is that formula (4.3), which is obtained by procedures which are valid only for $R \gg 1$, may be used to compute lobe Reynolds numbers for the spherical and cylindrical N-waves even when their Reynolds numbers are as small as $\frac{1}{2}$. Thus this formula can be used to determine the nature of the wave form in the non-planar cases and supplements the exact solution for plane N-waves given by Lighthill (1956).

The authors wish to thank Mr S. K. Sahni for programming the numerical scheme for IBM 360/65. This research was sponsored by the U.S. Air Force Office of Scientific Research under Grant 69-1687 B.

REFERENCES

Bateman, H. 1915 *Mon. Weather Rev.* **43**, 163.

Burgers, J. M. 1948 *Advances in Appl. Mech.* **1**, 171.

Cole, J. D. 1951 *Quart. Appl. Math.* **9**, 225.

Douglas, J. & Jones, B. V. 1963 *J. Soc. Ind. Appl. Math.* **11**. 195.

Hopf, E. 1950 *Commun. Pure Appl. Math.* **3**, 201.

Lighthill, M. J. 1956 *Surveys in Mechanics* (Ed. G. K. Batchelor & R. Davis), pp. 250–351. Cambridge University Press.

Leibovich, S. & Seebass, A. R. 1972 *Nonlinear Waves*, chap. 4. Cornell University Press (to appear).

Rusanov, V. V. 1961 *Zh. Nyck. Math.* **1**, 267.

Taylor, T. D., Ndefo, E. & Masson, B. S. 1972 *J. Comp. Phys.* **9**, 99.